An Efficient Method to Analyze the H-Plane Waveguide Junction Circulator with a Ferrite Sphere

Ru-Shan Chen, *Member IEEE,* and Edward Kai-Ning Yung, *Senior Member IEEE*

***Abstract*—This paper presents an approximate, but efficient field treatment of the new easy-to-fabricate ferrite-sphere-based H-plane waveguide circulator for potentially low-cost millimeter-wave communication systems. A new three-dimensional modeling strategy using a self-inconsistent mixed-coordinates-based mode-matching technique is developed, i.e., the solutions of the Helmholtz wave equations in the ferrite sphere and in the surrounding areas are deduced in the form of infinite summation of spherical, cylindrical, and general Cartesian modes, respectively. The point-matching method is then used on the interface between the ferrite sphere and air within the cylindrical junction, as well as the interface between the junction and waveguides to numerically obtain the coefficients of different orders of basis functions of the field. Therefore, the field distributions, as well as the characteristics of the circulator, are numerically calculated and good agreement is observed between the numerical results and measured data.**

***Index Terms*—Collocation method, eigenmode function, ferrite device, junction circulator, millimeter wave.**

I. Introduction

WAVEGUIDE Y-junction circulators have been widely used in microwave and millimeter-wave transmission and communication systems, although with the development of the monolithic-microwave integrated-circuit (MMIC) techniques, planar circulators have been utilized more and more in the microwave devices and circuits, the waveguide circulators still have their places in larger power cases. The H-plane waveguide junction circulators with a ferrite post of full or partial height have almost been studied thoroughly in theory and experiments. At millimeter-wave frequencies, however, the size of the ferrite post is too small to perform the fabrication and installation with precision, therefore, a novel waveguide Y-junction circulator with a ferrite sphere for millimeter waves application was proposed in [1] and [2]. However, the computer-aided design (CAD) [2] to model such a circulator made of this kind of ferrite sphere becomes very difficult because of a spherical topology that is not consistent with the rectangular waveguide coordinate.

Manuscript received February 12, 2000.

R.-S. Chen is with the School of Electronic Engineering and Photoelectrical Technology, Nanjing University of Science and Technology, Nanjing 210094, China.

E. K.-N. Yung is with the Wireless Communication Research Center, Department of Electronic Engineering, City University of Hong Kong, Kowloon, Hong Kong.

Publisher Item Identifier S 0018-9480(01)03318-X.

Since the 1960's, various methods have been developed for analysis and design of the waveguide Y-junction circulators with full-height ferrite posts [3]–[7]. Even though they are general for an arbitrarily shaped ferrite post, these analyses are limited to the circulators with full-height ferrite post. As for the circulator designed with a partial-height ferrite post, Owen [8] demonstrated that it operates in a turnstile fashion with rotating modes guided along the ferrite axis, and it also has a wider bandwidth as compared to its full-height counterpart. Although a number of approximate formulas have been given for engineering design [9]–[11], there is the lack of a rigorous theoretical model considering the realistic boundary conditions. The mode-matching analysis of a waveguide junction circulator with a partial-height ferrite post was presented [12]–[14], but the results do not agree well with the experiment. On the basis of simplified field expression [15], both volume and surface modes are used as eigenmodes to obtain $n = 2$ Chebyshev response related characteristics [16], [17]. Nevertheless, the analyses are still restricted to the case of a partial-height ferrite post.

In our case, the permeability tensor and spherical coordinate make it impossible to find a closed-form analytical expression of fields inside a magnetized ferrite sphere. Moreover, the self-inconsistent three coordinates (rectangular, cylindrical, and spherical) involved in an Y-junction waveguide circulator with a ferrite sphere give rise to an additional difficulty in handling its boundary condition in the analysis. Although a technique that is based on the equivalent principle and cavity field expansion [18], [19] was proposed to model the waveguide junction having an arbitrarily shaped anisotropic medium, hundreds of expanded functions are required to achieve only less than 3% error in their full-height composite ferrite post circulators. In [2], the ferrite sphere is approximated by bodies of revolution with segmented cross sections, whose surface is circumscribed by the spherical surface. The whole region in the Y-junction can be regarded as a composition of many annulus like [20] and [21], i.e., concentrically cascaded conducting parallel-plate cylindrical waveguides loaded with multiple layers containing dielectric (air) and ferrite medium in series. Matching tangential fields along every interfacial plane and applying the Galerkin technique lead to a set of solvable linear equations. Nevertheless, the whole analysis procedure seems a little complicated.

In this paper, a simpler simulation technique is presented, i.e., the electromagnetic fields in the ferrite sphere and in the surrounding areas are first expanded in the form of infinite summation of spherical, cylindrical, and general Cartesian modes, respectively. Also, the efficient and convenient point-matching

technique is then jointly used to model the H-plane millimeter-wave Y-junction circulator with a ferrite sphere. In Section II, the vector-scalar potential function is applied to the Maxwell equation having a permeability tensor, and a new divergence condition different from commonly used Coulomb's and Lorentz's conditions is proposed to get a scalar Helmholtz equation in spherical coordinates for spherical TE mode fields ($E_r = 0$). From the solutions of the equation, the presentations of the electromagnetic fields in the ferrite with the dc-biased magnetic field can be deduced. The surrounding area is divided into two parts: one is the junction area in which the fields are described in cylindrical coordinates, the other is the waveguide area with the Cartesian coordinate descriptions of the fields. The boundary between these two areas is an imaginary one, which may be a cylinder with the same axis as the waveguide junction. The presentations of the fields in the above three areas are in the form of infinite summations of spherical, cylindrical, and general Cartesian modes, respectively. Also, collocation technique is then applied to get a series of solvable equations for the magnitudes and phases of the electromagnetic-field components within the presentations. Results are presented in Section III, showing that the predicted insertion loss and isolation are in a fairly good agreement with the measured results since the ferrite loss is neglected in our model.

II. Theoretical Analysis

The configuration of an H-plane waveguide junction circulator with a ferrite sphere of radius R is sketched in Fig. 1. If the circulator is, for example, designed for uses in the 4-mm-wave range, it is fed by three WR12 waveguides of width 3.099 mm and of height 1.549 mm. The TE_{10} mode is the only mode of propagation in the waveguide. Gyrotropic Al–Ni–Zn ferrite spheres of relative permittivity $\varepsilon_r = 13.5$, of loss tangent $\sigma = 0.0005$, and of saturated magnetization $4\pi M_s = 4950$ G are selected. The radius of the ferrite sphere varies from 0.5 to 0.6 mm. It is fixed on top of a 0.2-mm-thick triangular impedance matching plate inside the waveguide junction. With the thickness of epoxy glue included, the sphere is approximately placed at the center of the waveguide junction. For easy reference, the circulator is placed on the x–y-plane. While Port 1 at $\phi = 0$ is designated as the input channel, Port 2 ($\phi = 2\pi/3$) and Port 3 ($\phi = 4\pi/3$) are output channels. The sphere is located in the center of the junction and magnetized in the z-direction by two electromagnets above and below the junction. The system is assumed to be free of losses and the output ports are perfectly matched, the exciting field is the rectangular dominant mode TE_{10}^x, and the time dependence of the electromagnetic-field components is in the form of $e^{j\omega t}$.

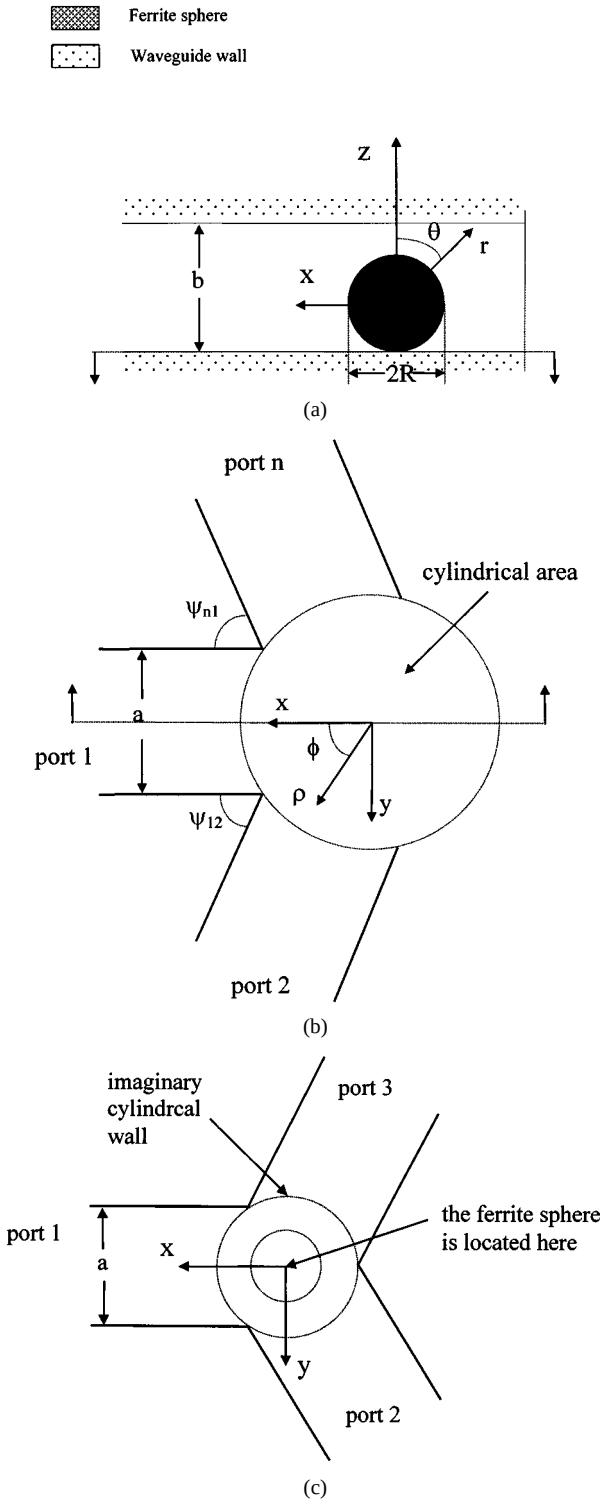

Fig. 1. (a) Section view on the center plane perpendicular to the wide side of the waveguide. (b) Section view on the bottom plane perpendicular to the narrow side of the waveguide. (c) Configuration of an H-plane waveguide Y-junction circulator with a ferrite sphere.

A. Field Presentation in the Ferrite Sphere

The origin of the spherical coordinate is selected at point $(0, 0, R)$ according to Fig. 1(c). The Maxwell equations in a nonconducting ferrite medium are as follows:

$$\nabla \times \vec{E} = -j\omega\mu_0[\mu_s]\vec{H} \tag{1}$$

$$\nabla \times \vec{H} = j\omega\varepsilon_0\varepsilon_{\mathrm{rf}}\vec{E} \tag{2}$$

$$\nabla \cdot \vec{D} = 0 \tag{3}$$

$$\nabla \cdot \vec{B} = 0 \tag{4}$$

where $[\mu_s]$ is the relative permeability tensor. If the ferrite medium is magnetized in the z-direction, $[\mu_s]$ in the spherical coordinates can be obtained by the following transformation:

$$[\mu_s] = [T][\mu_r][T]^{-1} \tag{5}$$

where

$$[\mu_r] = \mu_0 \begin{bmatrix} \mu & j\kappa & 0 \\ -j\kappa & \mu & 0 \\ 0 & 0 & \mu_z \end{bmatrix}$$

andthe transformation matrix $[T]$ is

$$[T] = \begin{bmatrix} \sin\theta\cos\phi & \sin\theta\sin\phi & \cos\theta \\ \cos\theta\cos\phi & \cos\theta\sin\phi & -\sin\theta \\ -\sin\phi & \cos\phi & 0 \end{bmatrix}.$$

For easy reference, $[\mu_s]$ is explicitly as follows:

$$[\mu_s] = \mu_0 \begin{bmatrix} \mu\sin^2\theta + \mu_z\cos^2\theta & (\mu-\mu_z)\sin\theta\cos\theta & j\kappa\sin\theta \\ (\mu-\mu_z)\sin\theta\cos\theta & \mu\cos^2\theta + \mu_z\sin^2\theta & j\kappa\cos\theta \\ -j\kappa\sin\theta & -j\kappa\cos\theta & \mu \end{bmatrix}. \tag{6}$$

It is interesting to note that $[\mu_s]$ is independent of φ, where

$$\mu = 1 + \frac{\omega_0\omega_m}{\omega_0^2 - \omega^2}$$
$$\kappa = \frac{\omega\omega_m}{\omega_0^2 - \omega^2} \tag{7}$$

and $\omega_0 = \mu_0\gamma H_0$ is the precession frequency, $\omega_m = \mu_0\gamma M_s$ is the characteristic parameter of the ferrite medium, ω is the operating frequency of the circulator, H_0 is the dc-bias magnetic field, M_s is the saturated magnetization of the ferrite material, and $\gamma = 1.758796 \times 10^{11}$ rad/T $\cdot$ s is the gyromagnetic ratio.

Since $\varepsilon_{\rm rf}$ of commonly used ferrite material is constant, from (3), we may have

$$\vec{E} = -\frac{1}{\varepsilon_0\varepsilon_{\rm rf}} \nabla \times \vec{A}. \tag{8}$$

In the free ferrite medium, if we substitute (8) into (2), we have

$$\nabla \times (\vec{H} + j\omega\vec{A}) = 0. \tag{9}$$

We can then assume

$$\vec{H} = -j\omega\vec{A} - \nabla\varphi. \tag{10}$$

If we substitute (8) and (10) into (1), we have

$$\nabla \times \nabla \times \vec{A} = -j\omega\varepsilon_0\mu_0\varepsilon_{\rm rf}[\mu_s]\left(j\omega\vec{A} + \nabla\varphi\right). \tag{11}$$

Since $[\mu_s]$ is a tensor, the Coulomb's and Lorentz's conditions commonly used in the vector-scalar potential method are not suitable here to get a scalar Helmholtz equation, and we have to find a new condition to stipulate the relation between the vector potential $\vec{A}$ and the scalar potential φ.

As is well known, generally used ferrite materials are of isotropic multicrystal. The electromagnetic fields inside such a material sphere may be expressed in terms of TE and TM waves, relative to the radial direction. Also, no hybrid mode is needed in such an isotropic sphere surrounding by air in spherical coordinates. However, the situation varies if it magnetized and placed in a waveguide junction. It has been demonstrated in [1] that the center operating frequency is approximately equal to the $\rm TE_{111}$-mode resonant one of a ferrite sphere for a millimeter-wave circulator, as if the latter were a dielectric sphere resonator. Also, the lowest mode in the junction circulator is mode $\rm TE_{111}$ because the $\rm TE_{101}$ mode of the ferrite sphere does not provide a ϕ-dependent wave. When a ferrite sphere is being magnetized in waveguide junction, the field inside the ferrite sphere will undergo some changes. No major changes are expected because the boundary condition remains intact and the magnetization is weak for a high millimeter-wave band due to the limit of available ferrite materials. Although a single $\rm TE_{mn\ell}$ mode could not satisfy the tensor Maxwell's equations, a series of $\rm TE_{mn\ell}$ modes approximately could. The innovation in [1] is to search for a minimum combination of eigenmodes that could approximately satisfy the tensor Helmholtz wave equations. In this paper, a more accurate eigenmode function of a tensor wave equation is explored to improve the accuracy of solution obtained in [1]. Here, the vector-scalar potential function is used and a new divergence condition different from commonly used Coulomb's and Lorentz's conditions is proposed to get a scalar Helmholtz equation in spherical coordinates for spherical TE mode fields ($E_r = 0$). From the solutions of the equation, the presentations of the electromagnetic fields in the ferrite biased by the dc magnetic field can be deduced. Thus, from (8), we have

$$\vec{A} = \hat{r}f(r, \theta, \phi). \tag{12}$$

Also, in order to get a scalar Helmholtz equation of the function f, we may then define the new divergence condition as follows:

$$\nabla\varphi = -j\omega\vec{A} - \frac{1}{j\omega\varepsilon_0\mu_0\varepsilon_{\rm rf}}[\mu_s]^{-1}\left[\nabla(\nabla\cdot\vec{A}) + \left(k_f^2 + \frac{2}{r^2}\right)\vec{A}\right] \tag{13}$$

where

$$k_f^2 = \omega^2\varepsilon_0\mu_0\varepsilon_{\rm rf}\frac{\mu^2 - \kappa^2}{\mu} \tag{14}$$

$$\mu_1[\mu_{sf}]^{-1} = \begin{bmatrix} \mu_1\cos^2\theta + \mu\sin^2\theta & \mu_2\sin\theta\cos\theta & -j\kappa\sin\theta \\ \mu_2\sin\theta\cos\theta & \mu_1\sin^2\theta + \mu\cos^2\theta & -j\kappa\cos\theta \\ j\kappa\sin\theta & j\kappa\cos\theta & \mu \end{bmatrix} \tag{15}$$

where

$$\mu_1 = \mu^2 - \kappa^2 \quad \mu_2 = \kappa^2 - \mu^2 + \mu.$$

If we substitute (13) and (12) into (11), we can get

$$\frac{\partial^2 f}{\partial r^2} + \frac{2}{r}\frac{\partial f}{\partial r} + \frac{1}{r^2}\left(\frac{\partial^2 f}{\partial\theta^2} + \frac{\partial f}{\partial\theta}\,ctg\theta\right) + \frac{1}{r^2\sin^2\theta}\frac{\partial^2 f}{\partial\phi^2} + k_f^2 f = 0 \tag{16}$$

i.e.,

$$\left(\nabla^2 + k_f^2\right)f = 0. \tag{17}$$

Considering the ferrite sphere includes the origin and the axis z, the solution of (17) is

$$f = \tilde{J}_n(k_f r)P_n^m(\cos\theta)\left(a_{mn}\sin m\phi + b_{mn}\cos m\phi\right) \tag{18}$$

in spherical coordinates where

$$\tilde{J}_n(u) = \sqrt{\frac{\pi}{2u}}\, J_{n+1/2}(u) \tag{19}$$

which is the spherical Bessel's function of the first kind and P_n^m is an associated Legendre polynomial.

From the solution of (8), (10), (13), (15), and (18), we can deduce the field distributions in the ferrite sphere coordinates

$$E_r = 0 \tag{20}$$

$$E_\theta = \sum_{mn} -\frac{m}{\varepsilon_0 \varepsilon_{\rm rf} r \sin\theta}\, \tilde{J}_n(k_f r) P_n^m(\cos\theta) \cdot \left(a_{mn}\cos m\phi - b_{mn}\sin m\phi\right) \tag{21}$$

$$E_\phi = \sum_{mn} \frac{1}{\varepsilon_0 \varepsilon_{\rm rf} r}\, \tilde{J}_n(k_f r) \frac{d}{d\theta}\left[P_n^m(\cos\theta)\right] \cdot \left(a_{mn}\sin m\phi + b_{mn}\cos m\phi\right) \tag{22}$$

$$\begin{aligned} H_r = \sum_{mn} & -\frac{j\omega}{\mu k_f^2 r} \cdot \Bigg\{ \Bigg[\frac{n(n+1)\left(\mu_1\cos^2\theta + \mu\sin^2\theta\right)}{r} \cdot \tilde{J}_n(k_f r) P_n^m(\cos\theta) a_{mn} \\ & + \Bigg[\mu_2 \sin\theta\cos\theta \frac{d}{d\theta}\left[P_n^m(\cos\theta)\right] a_{mn} + jm\kappa P_n^m(\cos\theta) b_{mn} \Bigg] \cdot \frac{d}{dr}\left[\tilde{J}_n(k_f r)\right] \sin m\phi \\ & + \Bigg[\frac{n(n+1)\left(\mu_1\cos^2\theta + \mu\sin^2\theta\right)}{r} \cdot \tilde{J}_n(k_f r) \cdot P_n^m(\cos\theta) b_{mn} \\ & + \Bigg[\mu_2 \sin\theta\cos\theta \frac{d}{d\theta}\left[P_n^m(\cos\theta)\right] b_{mn} - jm\kappa P_n^m(\cos\theta) a_{mn} \Bigg] \cdot \frac{d}{dr}\left[\tilde{J}_n(k_f r)\right] \cos m\phi \Bigg\} \end{aligned} \tag{23}$$

$$\begin{aligned} H_\theta = \sum_{mn} & -\frac{j\omega}{\mu k_f^2 r} \cdot \Bigg\{ \Bigg[\frac{n(n+1)\mu_2 \sin\theta\cos\theta}{r}\, \tilde{J}_n(k_f r) P_n^m(\cos\theta) a_{mn} \\ & + \Bigg[\left(\mu_1\sin^2\theta + \mu\cos^2\theta\right) \frac{d}{d\theta}\left[P_n^m(\cos\theta)\right] a_{mn} + jm\kappa ctg\theta P_n^m(\cos\theta) \cdot b_{mn} \Bigg] \cdot \frac{d}{dr}\left[\tilde{J}_n(k_f r)\right] \Bigg] \sin m\phi \\ & + \Bigg[\frac{n(n+1)\mu_2 \sin\theta\cos\theta}{r} \cdot \tilde{J}_n(k_f r) P_n^m(\cos\theta) b_{mn} \\ & + \Bigg[\left(\mu_1\sin^2\theta + \mu\cos^2\theta\right) \frac{d}{d\theta}\left[P_n^m(\cos\theta)\right] b_{mn} - jm\kappa ctg\theta P_n^m(\cos\theta) a_{mn} \Bigg] \cdot \frac{d}{dr}\left[\tilde{J}_n(k_f r)\right] \Bigg] \cos m\phi \Bigg\} \end{aligned} \tag{24}$$

$$\begin{aligned} H_\phi = \sum_{mn} & -\frac{j\omega}{\mu k_f^2 r} \cdot \Bigg\{ \Bigg[\frac{jn(n+1)\kappa\sin\theta}{r}\, \tilde{J}_n(k_f r) P_n^m(\cos\theta) a_{mn} \\ & + \Bigg[j\kappa\cos\theta \frac{d}{d\theta}\left[P_n^m(\cos\theta)\right] a_{mn} - \frac{m\mu}{\sin\theta} P_n^m(\cos\theta) b_{mn} \Bigg] \cdot \frac{d}{dr}\left[\tilde{J}_n(k_f r)\right] \Bigg] \sin m\phi \\ & + \Bigg[\frac{jn(n+1)\kappa\sin\theta}{r}\, \tilde{J}_n(k_f r) P_n^m(\cos\theta) \cdot b_{mn} \\ & + \Bigg[j\kappa\cos\theta \frac{d}{d\theta}\left[P_n^m(\cos\theta)\right] b_{mn} + \frac{m\mu}{\sin\theta} P_n^m(\cos\theta) a_{mn} \Bigg] \cdot \frac{d}{dr}\left[\tilde{J}_n(k_f r)\right] \Bigg] \cos m\phi \Bigg\}. \end{aligned} \tag{25}$$

Since the ferrite sphere is placed inside an H-plane millimeter-wave waveguide junction and the incident wave coming from the input rectangular waveguide is in the TE_{10} mode, the field in the ferrite sphere around the center operating frequency is mainly excited existing in the form of TE_{mnl} modes. The influence of the TM_{mnl} mode is neglected without bringing large error in our analysis.

B. Field Presentations in Surrounding Areas

Junction Area: Since the z-axis and origin are included in the region we want to consider, $z = 0$ and $z = b$ are electric walls, we may have the following presentations of the electromagnetic fields:

$$\begin{aligned} E_\rho = & \sum_{pq} \Bigg\{ \Bigg[-k_z \frac{d}{d\rho}\left[J_p(T\rho)\right] c_{pq} + \frac{j\omega\mu_0\mu_r p}{\rho} J_p(T\rho) f_{pq} \Bigg] \sin p\phi \\ & - \left[k_z \frac{d}{d\rho}\left[J_p(T\rho)\right] d_{pq} + \frac{j\omega\mu_0\mu_r p}{\rho} J_p(T\rho) e_{pq} \right] \cdot \cos p\phi \Bigg\} \sin k_z z \end{aligned} \tag{26}$$

$$\begin{aligned} E_\phi = & \sum_{pq} \Bigg\{ \Bigg[\frac{k_z p}{\rho} J_p(T\rho) d_{pq} + j\omega\mu_0\mu_r \frac{d}{d\rho}[J_p(T\rho)] e_{pq} \Bigg] \sin p\phi \\ & - \left[\frac{k_z p}{\rho} J_p(T\rho) c_{pq} - j\omega\mu_0\mu_r \frac{d}{d\rho}[J_p(T\rho)] f_{pq} \right] \cdot \cos p\phi \Bigg\} \sin k_z z \end{aligned} \tag{27}$$

$$E_z = \sum_{pq} T^2 J_p(T\rho)\left[c_{pq}\sin p\phi + d_{pq}\cos p\phi\right] \cos k_z z \tag{28}$$

$$\begin{aligned} H_\rho = & \sum_{pq} \Bigg\{ \Bigg[-\frac{j\omega\varepsilon_0\varepsilon_r p}{\rho} J_p(T\rho) d_{pq} + k_z \frac{d}{d\rho}\left[J_p(T\rho)\right] e_{pq} \Bigg] \sin p\phi \\ & + \left[\frac{j\omega\varepsilon_0\varepsilon_r p}{\rho} J_p(T\rho) c_{pq} + k_z \frac{d}{d\rho}\left[J_p(T\rho)\right] f_{pq} \right] \cdot \cos p\phi \Bigg\} \cos k_z z \end{aligned} \tag{29}$$

$$H_\phi = \sum_{pq}\Bigg\{-\left[j\omega\varepsilon_0\varepsilon_r\frac{d}{d\rho}[J_p(T\rho)]c_{pq}+\frac{k_z p}{\rho}J_p(T\rho)f_{pq}\right]\sin p\phi - \left[j\omega\varepsilon_0\varepsilon_r\frac{d}{d\rho}[J_p(T\rho)]d_{pq}-\frac{k_z p}{\rho}J_p(T\rho)e_{pq}\right]\cdot\cos p\phi\Bigg\}\cos k_z z \tag{30}$$

$$H_z = \sum_{pq} T^2 J_p(T\rho)\left[e_{pq}\sin p\phi + f_{pq}\cos p\phi\right]\sin k_z z \tag{31}$$

where

$$k_z = \frac{q\pi}{b} \quad T^2 = \omega^2\varepsilon_0\mu_0\varepsilon_r\mu_r - k_z^2. \tag{32}$$

Waveguide Area: Assuming the exciting field in waveguide port 1 is the waveguide dominant TE_{10} mode

$$E_x = E_y = H_z = 0 \tag{33}$$

$$E_z = -j\omega\mu_0\mu_r k_{y1}\cos(k_{y1}y)e^{jk_{x1}x} \tag{34}$$

$$H_x = -k_{y1}^2\sin(k_{y1}y)e^{jk_{x1}x} \tag{35}$$

$$H_y = -j\omega k_{x1}k_{y1}\cos(k_{y1}y)e^{jk_{x1}x} \tag{36}$$

where

$$k_{x1} = \sqrt{\omega^2\varepsilon_0\mu_0\varepsilon_r\mu_r - k_{y1}^2} \quad k_{y1} = \frac{\pi}{a}. \tag{37}$$

Due to the discontinuity of the junction and ferrite sphere, the incident field above induces the scattered fields in three waveguide ports in dominant and higher order modes, among which, all except dominant TE_{10} mode are cut off. The scattered fields in the ith waveguide can be written as

$$E_{xi} = \sum_{st}\left(k_y^2+k_z^2\right)g_{sti}\sin\left[k_y\left(y+\frac{a}{2}\right)\right]\sin(k_z z)e^{-jk_x x} \tag{38}$$

$$E_{yi} = \sum_{st} -j\left(k_x k_y g_{sti} - \omega\mu_0\mu_r k_z h_{sti}\right)\cdot\cos\left[k_y\left(y+\frac{a}{2}\right)\right]\sin(k_z z)e^{-jk_x x} \tag{39}$$

$$E_{zi} = \sum_{st} -j\left(k_x k_z g_{sti} + \omega\mu_0\mu_r k_y h_{sti}\right)\cdot\sin\left[k_y\left(y+\frac{a}{2}\right)\right]\cos(k_z z)e^{-jk_x x} \tag{40}$$

$$H_{xi} = \sum_{st}\left(k_y^2+k_z^2\right)h_{sti}\cos\left[k_y\left(y+\frac{a}{2}\right)\right]\cos(k_z z)e^{-jk_x x} \tag{41}$$

$$H_{yi} = \sum_{st} j\left(k_x k_y h_{sti} + \omega\varepsilon_0\varepsilon_r k_z g_{sti}\right)\cdot\sin\left[k_y\left(y+\frac{a}{2}\right)\right]\cos(k_z z)e^{-jk_x x} \tag{42}$$

$$H_{zi} = \sum_{st} j\left(k_x k_z h_{sti} - \omega\varepsilon_0\varepsilon_r k_y g_{sti}\right)\cdot\cos\left[k_y\left(y+\frac{a}{2}\right)\right]\sin(k_z z)e^{-jk_x x} \tag{43}$$

where

$$k_x = -j\sqrt{k_y^2+k_z^2-\omega^2\varepsilon_0\mu_0\varepsilon_r\mu_r} \quad k_y = \frac{s\pi}{a} \quad k_z = \frac{t\pi}{b} \tag{44}$$

and $s = 0, 1, 2, \ldots$, $t = 0, 1, 2, 3, \ldots$, but $s + t \neq 0$.

C. Matching Field on the Boundaries

We can use the tangential continuities of fields on the boundaries to obtain the coefficients in (20)–(25), (26)–(31), and (38)–(43). The first boundary is on the surface of the ferrite sphere, and the second is an imaginary one, the interface between the junction and the three waveguide arms.

Matching on the Surface of the Ferrite Sphere: The four boundary conditions on the surface of the ferrite sphere are

$$\begin{cases} E_{\phi\text{sphere}} = E_{\phi\text{cylinder}} \\ E_{\theta\text{sphere}} = E_{\rho\text{cylinder}}\cos\theta - E_{z\text{cylinder}}\sin\theta \\ H_{\phi\text{sphere}} = H_{\phi\text{cylinder}} \\ H_{\theta\text{sphere}} = H_{\rho\text{cylinder}}\cos\theta - H_{z\text{cylinder}}\sin\theta, \end{cases} \quad \text{when} \quad \begin{cases} r = R \\ \rho = R\sin\theta \\ z = R(1+\cos\theta). \end{cases} \tag{45}$$

Using the orthogonal properties of the trigonometric functions, substitute (20)–(25) and (26)–(31) into the right- and left-hand sides of (45), respectively, we have

$$\sum_n \frac{A_{e0}}{R}A2_{mn}(R,\theta)a_{mn} = \sum_q\left\{\frac{mk_z}{R\sin\theta}J_m(TR\sin\theta)d_{mq} + A_\mu T J_m'(TR\sin\theta)e_{mq}\right\}\cdot\sin\left[k_z R(1+\cos\theta)\right] \tag{46}$$

$$\sum_n \frac{A_{e0}}{R}A2_{mn}(R,\theta)b_{mn} = \sum_q\left\{-\frac{mk_z}{R\sin\theta}J_m(TR\sin\theta)c_{mq} + A_\mu T J_m'(TR\sin\theta)f_{mq}\right\}\sin\left[k_z R(1+\cos\theta)\right] \tag{47}$$

$$\sum_n \frac{mA_{e0}}{R\sin\theta}A1_{mn}(R,\theta)a_{mn} = \sum_q\Bigg\{\Bigg[-k_z T J_m'(TR\sin\theta)c_{mq} + \frac{mA_\mu}{R\sin\theta}\cdot J_m(TR\sin\theta)f_{mq}\Bigg]\sin\left[k_z R(1+\cos\theta)\right]\cos\theta - T^2 J_m(TR\sin\theta)\cdot c_{mq}\cos\left[k_z R(1+\cos\theta)\right]\sin\theta\Bigg\} \tag{48}$$

$$\sum_n -\frac{mA_{e0}}{R\sin\theta}A1_{mn}(R,\theta)b_{mn} = \sum_q \Big\{\Big[-k_zTJ'_m(TR\sin\theta)d_{mq} - \frac{mA_\mu}{R\sin\theta}\cdot J_m(TR\sin\theta)e_{mq}\Big]\sin\Big[k_zR(1+\cos\theta)\Big]\cos\theta - T^2J_m(TR\sin\theta)\cdot d_{mq}\cos\Big[k_zR(1+\cos\theta)\Big]\sin\theta\Big\} \quad (49)$$

$$\sum_n \frac{A_{h0}}{R}\Big\{\Big[-\frac{n(n+1)}{R}\mu_{13}(\theta)A1_{mn}(R,\theta) - \mu_{23}(\theta)\cdot A4_{mn}(R,\theta)\Big]a_{mn} - \frac{m\mu}{\sin\theta}A3_{mn}(R,\theta)b_{mn}\Big\} = \sum_q \Big\{-A_\varepsilon TJ'_m(TR\sin\theta)c_{mq} - \frac{mk_z}{R\sin\theta}\cdot J_m(TR\sin\theta)f_{mq}\Big\}\cos\Big[k_zR(1+\cos\theta)\Big] \quad (50)$$

$$\sum_n \frac{A_{h0}}{R}\Big\{\Big[-\frac{n(n+1)}{R}\mu_{13}(\theta)A1_{mn}(R,\theta) - \mu_{23}(\theta)\cdot A4_{mn}(R,\theta)\Big]b_{mn} + \frac{m\mu}{\sin\theta}A3_{mn}(R,\theta)a_{mn}\Big\} = \sum_q \Big\{-A_\varepsilon TJ'_m(TR\sin\theta)d_{mq} + \frac{mk_z}{R\sin\theta}\cdot J_m(TR\sin\theta)e_{mq}\Big\}\cos\Big[k_zR(1+\cos\theta)\Big] \quad (51)$$

$$\sum_n \frac{A_{h0}}{R}\Big\{\Big[\frac{n(n+1)}{R}\mu_{12}(\theta)A1_{mn}(R,\theta) + \mu_{22}(\theta)\cdot A4_{mn}(R,\theta)\Big]a_{mn} - \frac{m\mu_{23}(\theta)}{\sin\theta}A3_{mn}(R,\theta)b_{mn}\Big\} = \sum_q \Big\{\Big[-\frac{mA_\varepsilon}{R\sin\theta}J_m(TR\sin\theta)d_{mq} + k_zT\cdot J'_m(TR\sin\theta)e_{mq}\Big]\cos\Big[k_zR(1+\cos\theta)\Big]\cos\theta - T^2J_m(TR\sin\theta)e_{mq}\sin\Big[k_zR(1+\cos\theta)\Big]\sin\theta\Big\} \quad (52)$$

$$\sum_n \frac{A_{h0}}{R}\Big\{\Big[\frac{n(n+1)}{R}\mu_{12}(\theta)A1_{mn}(R,\theta) + \mu_{22}(\theta)\cdot A4_{mn}(R,\theta)\Big]b_{mn} + \frac{m\mu_{23}(\theta)}{\sin\theta}A3_{mn}(R,\theta)a_{mn}\Big\} = \sum_q \Big\{\Big[\frac{mA_\varepsilon}{R\sin\theta}J_m(TR\sin\theta)c_{mq} + k_zT\cdot J'_m(TR\sin\theta)f_{mq}\Big]\cos\Big[k_zR(1+\cos\theta)\Big]\cos\theta - T^2J_m(TR\sin\theta)f_{mq}\sin\Big[k_zR(1+\cos\theta)\Big]\sin\theta\Big\} \quad (53)$$

where

$$\begin{aligned} A_{e0} &= \frac{1}{\varepsilon_0\varepsilon_{\rm rf}} \\ A_{h0} &= -\frac{j\omega}{\mu k_f^2} \\ A_\varepsilon &= j\omega\varepsilon_0\varepsilon_r \\ A_\mu &= j\omega\mu_0\mu_r \end{aligned} \quad (54)$$

$$\begin{aligned} \mu_{11}(\theta) &= \mu_1\cos^2\theta + \mu\sin^2\theta \\ \mu_{12}(\theta) &= \mu_2\sin\theta\cos\theta \\ \mu_{13}(\theta) &= -j\kappa\sin\theta \\ \mu_{22}(\theta) &= \mu_1\sin^2\theta + \mu\cos^2\theta \\ \mu_{23}(\theta) &= -j\kappa\cos\theta \end{aligned} \quad (55)$$

$$A1_{mn}(R,\theta) = \tilde{J}_n(k_fR)P_n^m(\cos\theta) \quad (56)$$

$$A2_{mn}(R,\theta) = \tilde{J}_n(k_fR)\frac{d}{d\theta}\Big[P_n^m(\cos\theta)\Big] \quad (56)$$

$$A3_{mn}(R,\theta) = \frac{d}{dr}\Big[\tilde{J}_n(k_fR)\Big]P_n^m(\cos\theta)$$

$$A4_{mn}(R,\theta) = \frac{d}{dr}\Big[\tilde{J}_n(k_fR)\Big]\frac{d}{d\theta}\Big[P_n^m(\cos\theta)\Big]. \quad (57)$$

Since the different coordinates are used in the two sides of the boundary, complete mode matching cannot be achieved. Thus, a numerical technique must be used to get the solution, and it is available to obtain a unique solution only when the above conditions are combined with those on other boundary.

Matching on the Imaginary Boundary: As shown in Fig. 1(c), a cylindrical wall of radius $\rho = a/\sqrt{3}$, which has the same axis as the junction, is selected as the imaginary boundary, and the matching occurs on it. The boundary conditions on this wall can be given as following for the ith waveguide:

$$\begin{cases} E_{z\rm cylinder} = E_{z\rm iwaveguide} \\ E_{\phi\rm cylinder} = -E_{xi}\sin(\phi_i) + E_{yi}\cos(\phi_i)|_{\rm waveguide} \\ H_{z\rm cylinder} = H_{z\rm iwaveguide} \\ H_{\phi\rm cylinder} = -H_{xi}\sin(\phi_i) + H_{yi}\cos(\phi_i)|_{\rm waveguide}, \end{cases}$$

$$\text{when} \quad \begin{cases} \rho = a/\sqrt{3} \\ x_i = \dfrac{a}{\sqrt{3}}\cos\phi_i \\ y_i = \dfrac{a}{\sqrt{3}}\sin\phi_i \\ \phi_i = \phi - (2i-1)\dfrac{\pi}{3}. \end{cases} \quad (58)$$

Obviously, for any port, the value of ϕ_i is in $(-\pi/3, \pi/3)$. As previously treated in [4] and [5], we have

$$\sum_m T^2J_m\Big(\frac{Ta}{\sqrt{3}}\Big)\Big[c_{mq}\sin m\phi + d_{mq}\cos m\phi\Big] = -\delta_{0q}\delta_{1i}A_\mu k_{y1}\cos(k_{y1}y_i)\cdot e^{jk_{x1}x_i} - \sum_s \Big(jk_xk_zg_{sqi} + A_\mu k_yh_{sqi}\Big)A5_{sq}(\phi_i), \quad q = 0, 1, 2, \ldots \quad (59)$$

$$\sum_m T^2 J_m\left(\frac{Ta}{\sqrt{3}}\right)\left[e_{mq}\sin m\phi + f_{mq}\cos m\phi\right] = \sum_s \left(jk_x k_z h_{sqi} - A_\varepsilon k_y g_{sqi}\right) A6_{sq}(\phi_i), \quad q = 1, 2, 3, \ldots \tag{60}$$

$$\sum_m \left\{\left[B_{mq}d_{mq} + B_{m\mu}e_{mq}\right]\sin m\phi - \left[B_{mq}c_{mq} - B_{m\mu}f_{mq}\right]\cos m\phi\right\} = -\sum_s \left\{\left(k_y^2 + k_z^2\right) g_{sqi} A5_{sq}(\phi_i)\sin(\phi_i) + \left(jk_x k_y g_{sqi} - A_\mu k_z h_{sqi}\right) \cdot A6_{sq}(\phi_i)\cos(\phi_i)\right\}, \quad q = 1, 2, 3, \ldots \tag{61}$$

$$\begin{aligned}\sum_m \Bigg\{ &-\left[B_{m\varepsilon}c_{mq} + B_{mq}f_{mq}\right]\sin m\phi - \left[B_{m\varepsilon}d_{mq} - B_{mq}e_{mq}\right]\cos m\phi\Bigg\} \\ &= -\sum_s \Bigg\{\left(k_y^2 + k_z^2\right) h_{sqi} A6_{sq}(\phi_i)\sin(\phi_i) - \left(jk_x k_y h_{sqi} + A_\varepsilon k_z g_{sqi}\right) \cdot A5_{sq}(\phi_i)\cos(\phi_i)\Bigg\} \\ &\quad - \delta_{0q}\delta_{1i}\Bigg\{k_{y1}^2 \sin\left(k_{y1}y_i\right)\sin(\phi_i) + jk_{x1}k_{y1}\cdot\cos\left(k_{y1}y_i\right)\cos(\phi_i)\Bigg\} e^{jk_{x1}x_i}, \quad q = 0, 1, 2, \ldots\end{aligned} \tag{62}$$

where

$$\begin{aligned} B_{mq} &= \frac{\sqrt{3}mk_z}{a} J_m\left(\frac{Ta}{\sqrt{3}}\right) \\ B_{m\mu} &= A_\mu T J'_m\left(\frac{Ta}{\sqrt{3}}\right) \\ B_{m\varepsilon} &= A_\varepsilon T J'_m\left(\frac{Ta}{\sqrt{3}}\right) \end{aligned} \tag{63}$$

$$\begin{aligned} A5_{sq}(\phi_i) &= \sin\left[k_y\left(y_i + \frac{a}{2}\right)\right] e^{-jk_x x_i} \\ A6_{sq}(\phi_i) &= \cos\left[k_y\left(y_i + \frac{a}{2}\right)\right] e^{-jk_x x_i}. \end{aligned} \tag{64}$$

We know that s and t (now equal to q) are not permitted to be zero at same time. However, from above matching procedure, if $s = 0$, then $t \neq 0$, and (46)–(53) and (59)–(62) will be a set of homogeneous equations; the solution set (i.e., the values of coefficients in the presentations of fields) has only zero elements. This means $s = 1, 2, \ldots$.

Now we have eight equations for each m on the surface of ferrite sphere and 12 equations for each q on the imaginary boundary. It must be noted that for $q = 0$, there are only six equations on the latter boundary. Also, $q = 0$ must be had in any matching cases for obtaining a unique set of nonzero values of the coefficients. Since the number of the unknown coefficients involved are infinite, getting a closed exact solution set is impossible, but, in principle, we can get any degree accurate results by accounting for more than enough of spherical, cylindrical, and waveguide modes. Let us consider N_s spherical modes, N_c cylindrical modes, N_w waveguide modes in each waveguide, and N_{sc} matching points on the surface of the ferrite sphere, $N_{\rm cw}$ points on the imaginary boundary in each waveguide, the number of the total unknowns is then $2N_s + 4N_c + 6N_w$, and the number of the total equations is then $8(M-1)N_{sc} + (12Q+6)N_{\rm cw}$. The condition for obtaining the unique solution is

$$2N_s + 4N_c + 6N_w = 8(M-1)N_{sc} + (12Q+6)N_{\rm cw} \tag{65}$$

where

$$\begin{cases} N_s = \dfrac{(M-1)(2N-M)}{2} \\ N_c = (M-1)(Q+1) \\ N_w = S(Q+1) \end{cases} \qquad \begin{cases} m = 2, 3, \ldots, M \le N \\ n = 2, 3, \ldots, N \\ s = 1, 2, \ldots, S \\ q = 0, 1, \ldots, Q. \end{cases} \tag{66}$$

D. Performance of the Waveguide Junction Circulator

The input and output power density flow along the waveguides can be written in the following form:

$$P = \int_s \mathrm{Re}\left[\frac{1}{2}\vec{E} \times \vec{H}^*\right] \cdot d\vec{S}. \tag{67}$$

The input power density flow only exits in port 1 as follows:

$$P_{\rm in1} = -\frac{ab}{4}\omega\mu_0\mu_r k_{x1} k_{y1}^2 \tag{68}$$

where the minus sign denotes that the flow is opposite to the x-direction.

The output power density flow occurs in three waveguides as follows:

$$\begin{aligned} P_{{\rm out}i} = \frac{ab}{8}\sum_{sq}\Bigg\{ &\frac{2}{2^{1-\delta_{q0}}}\left(k_x k_z g_{sqi} - jA_\mu k_y h_{sqi}\right) \cdot \left(k_x k_y h_{sqi} - jA_\varepsilon k_z g_{sqi}\right) - (1-\delta_{q0}) \\ &\cdot \left(k_x k_y g_{sqi} + jA_\mu k_z h_{sqi}\right) \cdot \left(k_x k_z h_{sqi} + jA_\varepsilon k_y g_{sqi}\right)\Bigg\} \end{aligned} \tag{69}$$

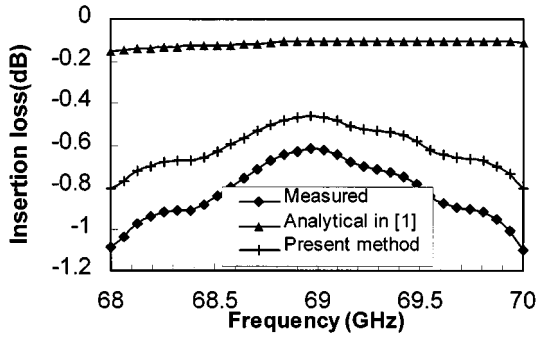

Fig. 2. Variation of the insertion loss of the circulator with frequency.

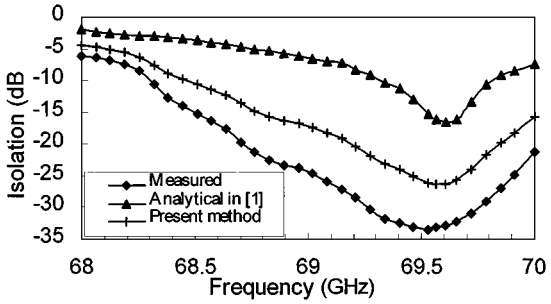

Fig. 3. Variation of the isolation of the circulator with frequency.

and the circulator characteristics (the power reflection coefficient η at port 1, the insertion loss τ at port 2, and the isolation α at port 3) can then be given as follows:

$$\eta = 10\log\left(\frac{P_{\text{out1}}}{P_{\text{in1}}}\right)$$
$$\tau = 10\log\left(\frac{P_{\text{out2}}}{P_{\text{in1}}}\right)$$
$$\alpha = 10\log\left(\frac{P_{\text{out3}}}{P_{\text{in1}}}\right). \tag{70}$$

III. Numerical Results and Discussions

The equations derived in the preceding section are now solved for characterizing the ferrite-sphere-based junction circulator. The choice of a finite number of matching points leads to a finite number of coupled (simultaneous) inhomogeneous equations and, the infinite expanded series involved in the equations representing sphere, waveguide, and cylindrical modes also have to be truncated for numerical calculations. These two requirements should guarantee the results accuracy within the following criteria: 1) the output power coming out of the three ports, i.e., the reflected power from the input port and the output power from the other two ports should equal the incident power. 2) A rapid convergence of the finite expanded series should be observed. This can be done by first selecting a specific number of the matching points and then obtaining certain mode amplitudes, then increasing the matching point number and observing the difference between the two consecutive calculations of the mode amplitudes. If the difference is negligible, the matching points are considered sufficient.

Variation of the insertion loss τ is plotted in Fig. 2 for 68 GHz $< f <$ 70 GHz. Experimental and analytical results in [1] are also included in Fig. 2 for comparison. Within the frequency band of interest, the insertion loss of our numerical technique is more closely approaching to experiment. A deviation of over 0.5 dB between the analytical prediction of [1] and the measurement is observed. This is expected because the reflection at the interface between the waveguide and waveguide junction, the reflection due to the impedance-matching patch, and the reflection on the surface of the ferrite sphere has not been considered for calculation in [1]. However, reflection at the interface between the waveguides and junction, as well as that on the surface of the ferrite sphere, has been considered for calculation in our developed method. Variation of the isolation α with respect to f is also sketched in Fig. 3. Although the shape of the analytical curve obtained in [1] is close to that of the experimental plot, the measured insertion loss is, on the average, twice as high as that predicted by the formula. This discrepancy is probably not only due to the omission of energy losses inside the waveguide junction, matching plate, epoxy glue, and ferrite sphere. It is mainly brought up due to neglecting the boundary conditions on the ferrite sphere surface, as well as the interface between three rectangular input/output waveguides and the H-plane cylindrical junction. Therefore, considering these two boundary conditions, our developed numerical approach in this paper obtains closer results to the experiment. Nevertheless, as the first attempt [1] to derive a simple method to analyze this cir-

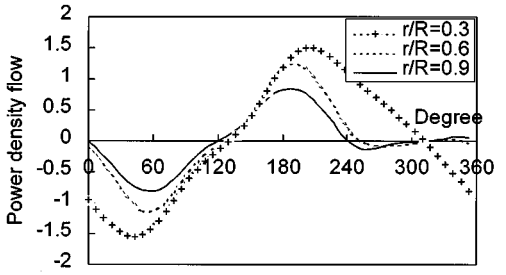

(a)

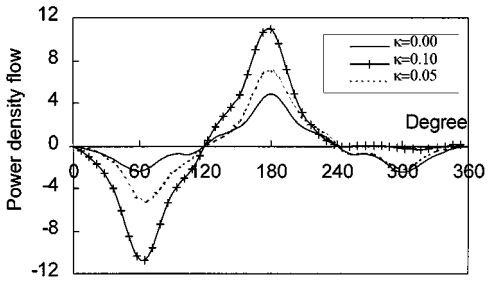

(b)

Fig. 4. (a) Normalized radial power-density flow profile $vs\phi$ at different radii r in the equatorial plane of ferrite-sphere-based H-plane Y-junction $R = a/\sqrt{3}$. (b) Normalized radial power-density flow profile $vs\phi$ for an off-diagonal element κ of permeability tensor at radii $r = 0.9R$ in the equatorial plane of ferrite-sphere-based H-plane Y-junction $R = a/\sqrt{3}$.

culator, the observed agreement of a center operating frequency should be accepted as satisfactory. For more accurate knowledge of insertion loss and isolation, the rigorous numerical technique developed in this paper should be adopted.

To understand the circulating mechanism better, the calculation of a power density flow in the radial direction of the Y-junction is desirable, which is defined simply by $\vec{P}_r = (1/2)\mathrm{Re}(\vec{E} \times \vec{H}^*) \cdot \vec{n}$, where $\vec{n}$ is unit vector in the radial direction. Fig. 4(a) plots the power density flow as a function of φ in the junction area. It denotes that, as r/R approaches one in the isolated port ($\varphi = 240°$–$360°$), $\vec{P}_r$ is approximately zero. The signal power injected into the input port ($\varphi = 120°$–$240°$) is almost completely transmitted into the output port ($\varphi = 0°$–$120°$), thereby achieving the circulating function. In addition, the power density flowing into the input port is positive, while it remains negative at the output port. This is normal in relation to the signal-flow orientation. The input and output power density flow in a closed cycle at any radius (air or ferrite region) is always balanced and conserved. This fact is expected, as the ferrite is considered lossless in our analysis and no power is dissipated inside the Y-junction area. On the other hand, an adequate choice of an off-diagonal element, as shown in Fig. 4(b), is also important for the circulator operation that can be readily optimized.

IV. Conclusion

A novel H-plane waveguide Y-junction circulator with a ferrite sphere has been designed for use in the 4-mm-wave range. A tiny ferrite sphere has been used to replace a ferrite cylinder because the sphere can be easily manufactured as if it were a ball bearing. With an insertion loss of less than 1 dB and an isolation of more than 20 dB in the frequency range of 68.7–70.1 GHz, the performance of this circulator has been comparable to the conventional circulator with a cylindrical ferrite. A simpler numerical simulation strategy has been given to determine the characteristic of ferrite-sphere-based waveguide circulator. Instead of discretizing the ferrite sphere into a lot of concentrically cascaded ferrite annulus adopted in [2], a faster and simpler TE_{mnl} eigenmode expansion method has been developed to evaluate various properties of a millimeter-wave circulator with a ferrite sphere considering the ferrite sphere placed in the H-plane waveguide junction. Since more applications of ferrite spheres in sub-millimeter waves or opto-electronics are envisaged, considering making a tiny perfect sphere is easier than producing a cylinder, the numerical technique developed in this paper is profound.

References

[1] E. K. N. Yung *et al.*, "A novel waveguide Y-junction circulator with a ferrite sphere for millimeter waves," *IEEE Trans. Microwave Theory Tech.*, vol. 44, pp. 454–45, Mar. 1996.

[2] E. K. N. Yung, R. S. Chen, and K. Wu, "Analysis and development of millimeter-wave waveguide junction circulator with a Ferrite sphere," *IEEE Trans. Microwave Theory Tech.*, vol. 46, pp. 1721–1734, Nov. 1998.

[3] J. B. Davies, "An analysis of the m-port symmetrical H-plane waveguide junction with central ferrite post," *IEEE Trans. Microwave Theory Tech.*, vol. MTT-10, pp. 596–604, Nov. 1962.

[4] M. E. El-Shandwily, A. A. Kamal, and E. A. F. Abdallah, "General field theory treatment of H-plane waveguide junction circulators," *IEEE Trans. Microwave Theory Tech.*, vol. MTT-21, pp. 392–403, June 1973.

[5] A. Khilla and I. Wolff, "Field theory treatment of H-plane waveguide junction with triangular ferrite post," *IEEE Trans. Microwave Theory Tech.*, vol. MTT-26, pp. 279–287, Apr. 1978.

[6] N. Okamoto, "Computer-aided design of H-plane waveguide junctions with full-height ferrites of arbitrary shape," *IEEE Trans. Microwave Theory Tech.*, vol. MTT-27, pp. 315–321, Apr. 1979.

[7] M. Koshba and M. Suzuki, "Finite-element analysis of H-plane waveguide junction with arbitrarily shaped ferrite post," *IEEE Trans. Microwave Theory Tech.*, vol. MTT-34, pp. 103–109, Jan. 1986.

[8] B. Owen, "The identification of modal resonances in Ferrite loaded waveguide Y-junction and their adjustment for circulation," *Bell Syst. Tech. J.*, vol. 51, no. 3, pp. 595–627, 1972.

[9] J. Helszajn *et al.*, "Design data for radial waveguide circulators using partial height Ferrite resonators," *IEEE Trans. Microwave Theory Tech.*, vol. MTT-23, pp. 288–298, Mar. 1975.

[10] J. Helszajn *et al.*, "Resonant frequencies, Q-factor, and susceptance slope parameter of waveguide circulators using weakly magnetized open resonators," *IEEE Trans. Microwave Theory Tech.*, vol. MTT-31, pp. 434–441, June 1983.

[11] J. Helszajn, "Design of waveguide circulators with Chebyshev characteristics using partial height Ferrite resonators," *IEEE Trans. Microwave Theory Tech.*, vol. MTT-32, pp. 908–917, Aug. 1984.

[12] EL-Shandwily *et al.*, "General field theory treatment of E-plane waveguide junction circulators N—Part I: Full-height Ferrite configuration," *IEEE Trans. Microwave Theory Tech.*, vol. MTT-25, pp. 784–793, Sept. 1977.

[13] EL-Shanclwily *et al.*, "General field theory treatment of E-plane waveguide junction circulators N—Part II: Two disk Ferrite configurations," *IEEE Trans. Microwave Theory Tech.*, vol. MTT-25, pp. 794–803, Sept. 1977.

[14] Y. Akaiwa, "A numerical analysis of waveguide H-plane Y junction circulators with circular partial height Ferrite post," *Trans. Inst. Electron. Inf. Commun. Eng. E*, vol. 61, no. 8, pp. 609–617, Aug. 1978.

[15] W. Hauth, "Analysis of circular waveguide cavities with partial height Ferrite insert," in *Proc. European Microwave Conf.*, 1981, pp. 383–388.

[16] W. B. Dou and S. F. Li, "On volume modes and surface modes in partial height Ferrite circulators and their bandwidth expansion at millimeter wave band," *Microwave Opt. Technol. Lett.*, vol. 1, no. 6, pp. 200–208, Aug. 1988.

[17] W. B. Don and Z. L. Sun, "Millimeter wave Ferrite circulators and rotators," *Int. J. Infrared Millim. Waves*, vol. 17, no. 12, pp. 2034–2131, Dec. 1996.

[18] Y. Y. Tsai and A. S. Omar, "Field theoretical treatment of E-plane waveguide junctions with anisotropic medium," *IEEE Trans. Microwave Theory Tech.*, vol. 40, pp. 2164–2171, Dec. 1992.

[19] ——, "Field theoretical treatment of H-plane waveguide junctions with anisotropic medium," *IEEE Trans. Microwave Theory Tech.*, vol. 41, pp. 274–281, Feb. 1993.

[20] W. K. Hui and I. Wolff, "A multicomposite multilayered cylindrical dielectric resonator for application in MMIC," *IEEE Trans. Microwave Theory Tech.*, vol. 42, pp. 415–423, Mar. 1994.

[21] C. M. Krowne and R. E. Neidert, "Theory and numerical calculation for radially inhomogeneous circuit Ferrite circulators," *IEEE Trans. Microwave Theory Tech.*, vol. 44, pp. 419–431, Mar. 1996.

Ru-Shan Chen (M'95) was born in Jiangsu, China, He received the B.Sc. and M.Sc. degrees from the Southeast University, Nanjing, China, in 1987 and 1990, respectively, both in radio engineering.

He then joined the Department of Electrical Engineering, Nanjing University of Science and Technology (NUST), Nanjing, China, where he was initially a Teaching Assistant, and then, in 1992, a Lecturer. In September 1996, he was a Visiting Scholar with the Department of Electronic Engineering, City University of Hong Kong, initially as a Research Associate, then a Senior Research Associate in July 1997, and then a Research Fellow in April 1998. From June to September 1999, he was also a Visiting

Scholar at the Montreal University, Montreal, PQ, Canada. In September 1999, he became a full Professor and Associate Director of the Microwave and Communication Center, NUST. He has taught several courses, including "Computer Language and Algorithms," "Professional English," "Electromagnetic Field and Wave Theory," "Computational Electromagnetics," "Microwave Ferrite Theory and Applications," and "Electromagnetic Compatibility." He has authored or co-authored over 80 papers, including 42 published in international journals. His research interests mainly include microwave/millimeter-wave systems, measurements, antennas, circuits, and computational electromagnetics.

Dr. Chen was the recipient of the 1992 Third-Class Science and Technology Advance Prize presented by the National Military Industry Department of China, the 1993 Third-Class Science and Technology Advance Prize presented by the National Education Committee of China, the 1996 Second-Class Science and Technology Advance Prize presented by the National Education Committee of China, and the 1999 First-Class Science and Technology Advance Prize presented by JiangSu Province. While with NUST, he was the recipient of the Excellent Honor Prize for academic achievement (1994, 1996, 1997 and 1999).

Edward Kai-Ning Yung (M'85–SM'95) was born in Hong Kong. He received the B.Sc. degree in electrical engineering (with special distinction), and the M.S. and Ph.D. degrees from the University of Mississippi, University, in 1972, 1974, and 1977, respectively.

Upon graduation, he was briefly with the Electromagnetic Laboratory, the University of Illinois at Urbana-Champaign. In 1978, he joined the Hong Kong Polytechnic. In 1984, he joined the City University of Hong Kong, and was instrumental in setting up a new department. In 1989, he became a Full Professor, and in 1994, he was awarded one of the first two personal chairs at the University. He is the founding Director of the Wireless Communications Research Center (formerly the Telecommunications Research Center). He currently heads the Department of Electronic Engineering (the largest of its kind in Hong Kong). He remains active in research in microwave devices and antenna designs for wireless communications. He is also the principal investigator of many funded projects. He has authored over 120 papers in journals and has presented 140 papers in international conferences. He is also active in applied research, consultancy, and other types of technology transfers. He holds one patent. He is the external examiner of many graduate students in sister universities, both local and overseas. He is listed in the *Who's Who in the World* and *Who's Who in the Science and Engineering in the World*.

Dr. Yung is a Fellow of the Chinese Institution of Electronics, the Institute of Electrical Engineers (IEE), U.K. and the Hong Kong Institution of Engineers. He is a member of Eta Kappa Nu, Phi Kappa Phi, Tau Beta Pi, and the Electromagnetics Academy. He is currently the chairman of the Electronics Discipline, the Hong Kong Institution of Engineers. He was the elected president of the Hong Kong Association for the Advancement of Science and Technology (1998–1999), president of the Association of Experts for the Modernization of China (1989–1990 and 1998–1999), and vice president of the Hong Kong Institution of Engineers (1999–2000). He was the general chairman of many international conferences held in Hong Kong. He holds Honorary Professorships at two major universities in China. He has been the recipient of many awards in applied research, including the 1991 Texas Instrument Incorporated Design Championship Grand Prize, the 1998 Chinese International Invention Exposition Silver Medal, and the 1999 CMA Design Award. He also co-authored a paper that was awarded the 1996 Young Scientist Award presented at the IEEE International Symposium on Antennas and Propagation, Tokyo, Japan.